

Unambiguous quasar microlensing

Mark A. Walker

Special Research Centre for Theoretical Astrophysics, School of Physics, University of Sydney, NSW 2006, Australia

Accepted

. Received

ABSTRACT

Microlensing studies of quasars can reveal dark matter lumps over a broad mass spectrum; we highlight the importance of monitoring quasars which are seen through the halos of low-redshift galaxies. For these configurations microlensing by planetary-mass objects will manifest itself as isolated events which are only weakly chromatic. Statistical comparison of the observed optical depths with their theoretical counterparts provides a strong test for a microlensing origin of such events. If microlensing is detected, the light-curves can reveal not only the characteristic microlens masses, and their corresponding contribution to dark halos, but also how compact the individual objects are. In this way we can decisively test the possibility that the dark matter associated with galaxies is composed principally of planetary-mass gas clouds.

Key words: dark matter — gravitational lensing — quasars: general

1 INTRODUCTION

Flux monitoring of quasars has provided evidence that the dark matter might be composed of objects of planetary mass, $M \lesssim 10^{-3} M_{\odot}$. This evidence comes from two types of observations: optical variability that may be due to distant gravitational microlenses (Irwin et al. 1989; Hawkins 1993; Schild 1996); and radio monitoring data (Fiedler et al. 1987), which show “Extreme Scattering Events” (ESEs), can be sensibly interpreted as plasma lensing by cool clouds in the Galactic halo (Walker & Wardle 1998). However, these data can be interpreted in other ways (Wambsganss, Paczyński & Schneider 1990; Baganoff & Malkan 1995; Schmidt & Wambsganss 1998; Romani, Blandford and Cordes 1987), and the idea that dark matter takes the form of planetary mass lumps is currently just an interesting suggestion. What is needed now is to move away from suggestive evidence, which has served its purpose in drawing attention to the proposed picture, and towards some decisive observational tests. Such tests have previously been contemplated (Press & Gunn 1973; Gott 1981; Canizares 1982; Vietri & Ostriker 1983; Paczyński 1986), with firm negative results for some mass ranges (Press & Gunn 1973; Dalcanton et al. 1994; Carr 1994; Alcock et al. 1998). However, all of these tests admit the possibility of a substantial quantity of dark matter residing in planetary-mass gas-clouds. In view of the quasar monitoring data, observations designed specifically to investigate this particular mass range would be worthwhile. In this paper we demonstrate that clean experimental tests are, in fact, quite straightforward to arrange in respect of quasar microlensing. The most important consideration is selection of the sample of sources to be monitored; as described in §2 and §3, these should be apparently close to low redshift galaxies. In §4 we discuss the potential of such data for dis-

tinguishing between low-mass gas clouds and more compact microlenses.

2 MICROLENSING AT LOW OPTICAL DEPTH

The large-scale distribution of dark matter within a galaxy can be approximated by an isothermal sphere, for which the surface density as a function of radius, r , is (Gott 1981)

$$\Sigma(r) = \frac{\sigma^2}{2Gr}, \quad (1)$$

where σ is the line-of-sight velocity dispersion, and we have neglected the possibility of a core in the density distribution. Suppose now that this surface density is *entirely* in compact lumps of material (the meaning of “compact” will be addressed in §3), then it follows that the optical depth to gravitational microlensing by these lumps is just

$$\tau = \frac{\Sigma(r)}{\Sigma_c} = 2\pi \frac{\sigma^2}{c^2} \frac{1}{\chi}, \quad (2)$$

where $\Sigma_c \simeq c^2/4\pi GD_d$ is the critical surface density for multiple imaging, and $\chi \equiv r/D_d$, for a galaxy at distance D_d . Here we have assumed that we are observing a distant quasar behind a low-redshift galaxy. If, for simplicity, we suppose that all large galaxies can be approximated as having $\sigma \simeq 150 \text{ km s}^{-1}$, then we arrive at the convenient formulation

$$\tau \sim \frac{1}{3\chi}, \quad (3)$$

where χ is now expressed in arcseconds. From this we can see immediately that any quasar which lies within, say, an

arcminute of a bright galaxy stands a modest chance of being microlensed, providing only that the dark matter is in compact form.

A corollary of the above is that any quasar which is aligned within about an arcsecond of the centre of an intervening galaxy has near unit probability of being microlensed at any given time. So is such an alignment the most favourable place to investigate microlensing? No. This situation is favourable in only two respects: first there will very likely be macrolensing – i.e. multiple imaging of the quasar on the scale of arcseconds – which, by photometric monitoring of the individual macro-images, permits microlensing to be distinguished from variations which are intrinsic to the quasar. Secondly the large optical depth means that there will be essentially continuous microlensing variations. Unfortunately these benefits are offset by two substantial disadvantages: first the central arcsecond of any large galaxy is composed predominantly of stars, not dark matter; and secondly the network of caustics which occurs at high optical depths (see, for example, Schneider, Ehlers & Falco 1992) leads to complex light-curves which are difficult to interpret. (Note that it is not easy even to measure, accurately, the brightness of the individual macro-images, as they are blended with the core of the lensing galaxy, and with each other, in ground-based observations). Indeed these problems are evident in the literature on the gravitationally lensed quasar 2237+0305, which is seen through the central bulge of a low-redshift galaxy. Rapid variations in the flux of one of the macro-images were initially interpreted (Irwin et al 1989) in terms of microlensing by a low-mass object, but this interpretation was later challenged (Wambsganss, Paczyński & Schneider 1990) and the data re-interpreted in terms of microlensing by stars. Subsequently it has been emphasised that the light-curves for this system *do* admit a population of low-mass lenses (Refsdal & Stabel 1993), leaving the whole question quite open.

The difficulty of interpreting light-curves which arise from a dense network of caustics argues for a shift in emphasis towards monitoring of systems where the optical depth is small. In this regime we may observe individual microlensing events, superimposed on a more-or-less steady baseline (distinguishing microlensing from other forms of variability is addressed in §5). This is a great advantage in that the observed event time-scales can then be related more-or-less directly to mass scales. The lower event-rate associated with a small optical depth is the principal disadvantage of this regime, but this can be offset by studying a larger number of targets in order to accumulate good statistics.

3 MICROLENSING AT LOW REDSHIFT

So far we have given no reason to prefer galaxies in any particular redshift range. In constructing a sample of quasars seen through galaxy halos we would find that most of the cases involve distant galaxies, simply because there is a greater surface density of distant galaxies than nearby ones. Unfortunately these examples are less useful for investigating microlensing by low-mass objects; the reason is that at large distances the angular size of the (Einstein ring of the) lens becomes smaller than the angular size of the quasar, and so the apparent changes in quasar flux are small. If this happens we lose not only signal-to-noise ratio but also

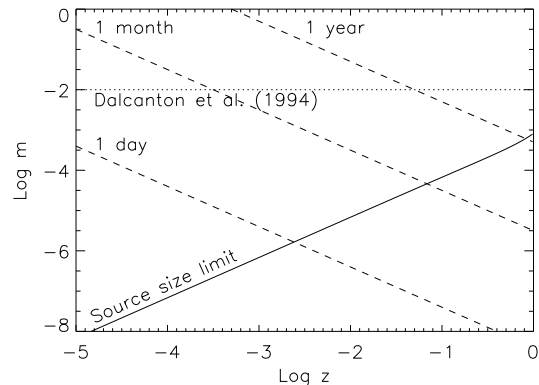


Figure 1. Detectability of gravitational microlensing by compact masses ($m \equiv M/M_{\odot}$) as a function of lens redshift, z . In order for a microlens to introduce significant magnification, it must be more massive than indicated by the “source-size limit”. The adopted source size is 10^{15} cm, located at $z_Q = 2$, and an empty ($\Omega = 0$) universe is assumed. Approximate time-scales for microlensing events are shown by the dashed lines (assuming a transverse speed of 600 km s^{-1}). The upper bound of Dalcanton et al. (1994) is also plotted: this corresponds to the largest permitted mass, if galaxy halos contribute $\Omega_g \sim 0.1$, are entirely composed of microlenses, and $\Omega < 0.6$.

our ability to predict light-curves, because our current understanding of the emission from quasars is so poor that the point-source approximation is the only one which enables confidence. (Of course, one can use lensing phenomena to investigate source structure, but that is not our concern here.) This is especially important because a resolved source may exhibit substantial differences between the light-curves seen at different frequencies, whereas microlensing events of a point-like source by a point-like lens are achromatic and this feature aids the interpretation of any observed variability.

Figure 1 illustrates the limits imposed by source size on the detectability of microlenses, of various masses, as a function of lens redshift. (We note here that the mass limits quoted by Walker & Ireland [1995] are too pessimistic – they appear to have been derived from a comparison between the linear dimensions, rather than the angular dimensions, of lens and source – thanks to Steve Warren for drawing attention to this.) To be definite we take a source of radius 10^{15} cm (c.f. Wambsganss, Paczyński & Schneider 1990) at $z_Q = 2$; we adopt a Hubble constant of $75 \text{ km s}^{-1} \text{ Mpc}^{-1}$, and angular-diameter/redshift relations appropriate to an $\Omega = 0$ universe. From figure 1 it is evident that for microlenses at $z_d \sim 1$ there will be relatively little sensitivity to the mass range $M \lesssim 10^{-3} M_{\odot}$. This is just the mass range of interest and so it is critical to select lines-of-sight which intersect *low-redshift* galaxies. For example, at $z_d \sim 10^{-2}$ we have sensitivity to microlenses of $M \gtrsim 10^{-5} M_{\odot}$, with the upper end of the mass range being fixed by the duration of the monitoring experiment. We note that if galaxies contribute $\Omega_g \sim 0.1$ to the cosmological density parameter, Ω , and $\Omega < 0.6$, then microlenses which are more massive than $10^{-2} M_{\odot}$ cannot dominate their halos (Dalcanton et al. 1994) — a result which follows from analysis of the equivalent widths of quasar emission lines. This bound is

plotted in figure 1. Approximate microlensing event time-scales are also plotted in figure 1, and from these we see an added advantage of low redshift galaxies, namely that the time-scales are well matched to an observing program. By contrast events involving $10^{-3}M_{\odot}$ microlenses take years at $z_d \sim 1$.

The considerations we have given also apply to the lowest redshift halo, namely the Galactic halo, which has a very small optical depth, $\tau < 10^{-6}$. Paczyński (1986) suggested that its compact constituents could be revealed by their microlensing influence on the flux from LMC stars. Indeed microlensing by stellar-mass objects has now been detected in this way (Alcock et al. 1997). Precisely because the observed lenses are stellar mass, however, there remains a concern that these signals are due to the known Galactic/Magellanic stellar populations (Sahu 1994), or to tidal debris (Zhao 1998), and are unrepresentative of the Galactic halo as a whole. This notion is reinforced by the Dalcanton et al. (1994) constraints, mentioned earlier. Significantly, no signal has been seen from planetary-mass objects (Alcock et al. 1998), which calls into question the microlensing interpretation of quasar variability. One possible resolution of this apparent conflict is that the low-mass microlenses suggested by Irwin et al. (1989), Hawkins (1993,1995) and Schild (1996) are not actually dense enough to be strong microlenses in the context of the Galactic halo, implying that their characteristic surface density lies in the range

$$0.1 \lesssim \Sigma(\text{g cm}^{-2}) \lesssim 10^4. \quad (4)$$

This range includes the estimated mean surface density of the individual gas clouds ($\sim 10^2 \text{ g cm}^{-2}$) in the model of Walker & Wardle (1998), but excludes black holes and planets. It is worth noting that *all* baryonic, Galactic dark matter candidates are required to have a characteristic surface density $\Sigma \gtrsim 3 \text{ g cm}^{-2}$, in order for them not to have collided with each other within the age of the Universe (Gerhard & Silk 1996). This implies that all baryonic dark matter candidates associated with galaxies must be strong gravitational lenses by $z_d \sim 0.03$.

An important point has recently been made by Draine (1998): dense gas clouds can act as strong lenses purely on account of the refractive index of the gas itself. Draine further notes that the optical light curves for *gas* microlensing events are very similar to those for *gravitational* microlensing (see also Henriksen and Widrow 1995), raising the startling possibility that some of the observed microlensing events might actually be due to gas lensing! At present predictions concerning gas lensing are limited primarily by our ignorance of the likely run of density within the putative clouds. But given any specific density distribution we can incorporate the refractive index of the gas in our calculation of lensing behaviour; this is the approach we shall take.

4 MICROLENSING BY GAS CLOUDS

In the previous sections we concentrated on the means by which one can best test the picture that dark matter takes the form of planetary mass lumps, with little regard for the specific nature of these lumps. The observations which we advocate can, however, tell us more than just the mass of any microlens: they also give us information on the surface

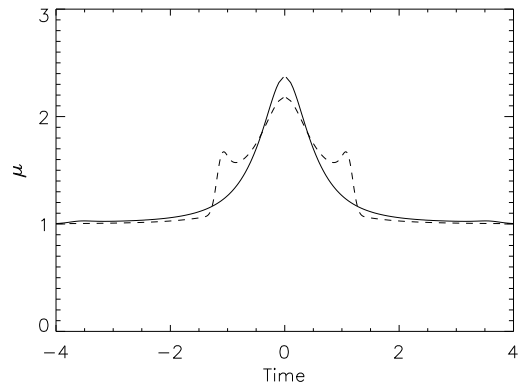


Figure 2. Model light-curves for lensing of a $z_Q = 2$ quasar by a $3 \times 10^{-4} M_{\odot}$ gas cloud, of $\Sigma_0 = 100 \text{ g cm}^{-2}$, at $z_d = 0.002$ (dashed line) and 0.01 (solid line). These correspond to $\kappa_0 = 2.3, 12$, respectively, while κ'_0 (describing refraction by the gas itself) is, in the optical band, roughly 30% larger than κ_0 in each case. The impact parameter for each event is taken to be 0.5 Einstein ring radii, and time is given in units of the crossing-time for one Einstein ring radius. The same source model is adopted as for figure 1.

density distribution of the individual lenses. At a crude level this is already obvious from our discussion in §3. On a more subtle level there are diagnostic features present in the light-curves even when the clouds are securely in the strong lensing regime (see also Henriksen & Widrow 1995). To demonstrate this we take the example of a Gaussian surface density profile for each microlens

$$\Sigma(r) = \Sigma_0 \exp(-r^2/2\sigma^2). \quad (5)$$

The corresponding mass is then $M = 2\pi\sigma^2\Sigma_0$. If we express all angles in units of the Einstein ring radius for this mass then we arrive at the lens equation which gives the image locations (θ) implicitly in terms of the source location (β):

$$\beta = \theta \left[1 - \kappa'_0 \exp(-\kappa_0\theta^2) \right] - \frac{1}{\theta} \left[1 - \exp(-\kappa_0\theta^2) \right]. \quad (6)$$

Here we have written $\kappa_0 \equiv \Sigma_0/\Sigma_c$ for the central surface density of the cloud in units of the critical surface density for multiple gravitational imaging; and similarly $\kappa'_0 \equiv \Sigma_0/\Sigma'_c$ where, following Draine (1998), and making use of his quantity α , $\Sigma'_c \simeq \sigma^2/\alpha D_d = M/2\pi\Sigma_0\alpha D_d$. In the optical band, $\alpha \simeq 1.2 \text{ cm}^3 \text{ g}^{-1}$, not strongly dependent on frequency (Draine 1998). In equation 6, then, the term in κ'_0 describes refraction by the gas.

There are two simple analytic limits of equation 6: for $\kappa_0\theta^2 \gg 1$ we recover the Schwarzschild lens mapping $\beta \simeq \theta - 1/\theta$, appropriate to the point-mass lens approximation; while at the other extreme ($\kappa_0\theta^2 \ll 1$) we have $\beta \simeq \theta(1 - \kappa_0 - \kappa'_0)$ as, indeed, we might expect (see Schneider, Ehlers & Falco, 1992, for discussion of these cases). The individual image magnifications are determined from $\mu = (\theta/\beta)\partial\theta/\partial\beta$, and so the light-curves corresponding to these lenses will evidently be very different. Of more interest, though, is the general case for which we require the exact mapping (equation 6). In figure 2 we show theoretical light-curves for clouds of mass $3 \times 10^{-4} M_{\odot}$, and central surface density $\Sigma_0 = 100 \text{ g cm}^{-2}$, at $z_d = 0.002, 0.01$. These curves

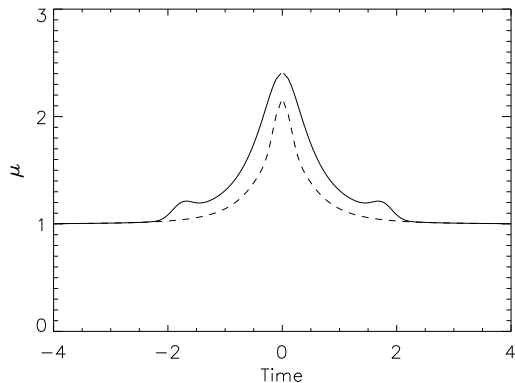


Figure 3. As figure 2, but with refraction by the gas neglected ($\kappa'_0 = 0$), so that lensing is entirely due to the gravitational field.

pertain to the optical band, where refraction by the gas itself contributes substantially (Draine 1998) — for our particular model $\kappa'_0 \simeq 4\kappa_0/3$. It is reasonable to anticipate that target quasars could be monitored with a standard error of 0.01 magnitudes, so the differences between these two light-curves are easily measurable. The more distant of the two examples is not quite distinguishable from a truly point-like lens. An important qualitative feature of each curve, which is not present for the Schwarzschild lens, is the existence of a fold caustic at $\theta \simeq 1/\sqrt{\kappa_0 + \kappa'_0}$. This caustic introduces a thin annulus of high magnification which, by virtue of its small angular extent, is expected to be chromatic even if the principal peak in the light-curve is not; this caustic is evident in figure 2 as the subsidiary peaks at $t \simeq \pm 1.2$ for the lower redshift lens. For the more distant lens the caustic crossing occurs at $t \simeq \pm 3.7$, but the high magnification region is so thin (in comparison with the source dimension) that there is no peak in the light-curve at these locations. For reference we show in figure 3 light-curves for our model clouds at wavelengths where there is negligible refraction by the gas itself (i.e. $\kappa'_0 \ll \kappa_0$). In figure 3 both light curves are readily distinguished from microlensing by a point-mass lens. Relative to figure 2, where refraction by the gas is non-negligible, the principal difference is that the caustic ring shrinks in radius, because of the smaller central “beam convergence” (sum of κ_0 and κ'_0), and becomes broader. For the more distant lens (solid line), the increased width of the annulus of high magnification renders the caustic more visible in figure 3 than figure 2. For the lower redshift lens, however, the source only grazes the caustic, rather than crossing it, and this leads to a single central peak in the light-curve.

A final point to make is that where light passes through a gas cloud some absorption may occur. This is expected to be a small effect in the optical band (else the putative clouds should have already been discovered in this way), but the extinction is certainly large in the far UV and throughout the X-ray region. X-ray light-curves are therefore expected to appear quite different to their optical counterparts, in cases where the lens is not point-like. To demonstrate this we have computed X-ray light-curves for our model clouds. At energies of several keV to several hundred keV the extinction is principally due to electron scattering, so across this broad range each cloud presents an optical

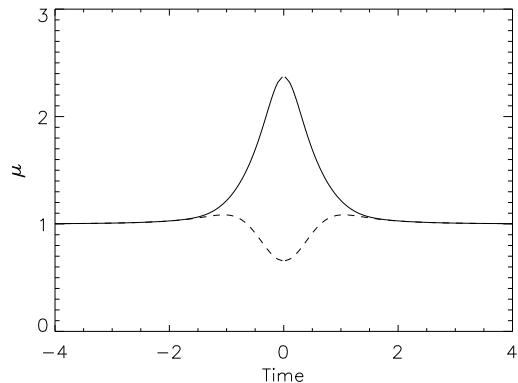


Figure 4. As figure 2, but with $\kappa'_0 = 0$, and adopting an opacity of $0.4 \text{ cm}^2 \text{ g}^{-1}$ — these values are appropriate to lensing in the hard X-ray band, where Thomson scattering dominates the opacity of the gas.

depth $\tau \simeq 40 \exp(-r^2/2\sigma^2) = 40 \exp(-\kappa_0\theta^2)$. Image locations are as given by equation 6, with $\kappa'_0 = 0$ (refraction by the gas is negligible in the X-ray band), and each image is attenuated by a factor $\exp(-\tau)$. The resulting light-curves are shown in figure 4; these curves may be compared directly with those of figure 2, which involve the same lensing geometry and differ only in observing wavelength. Interestingly, while the more distant lens has a light-curve which qualitatively still resembles microlensing by a point mass, the nearby lens ($z_d = 0.002$, dashed curve) manifests an extinction event. Now both lenses have the same physical optical depth profile, with a central optical depth of 40, so this difference is entirely a consequence of the different lensing geometries. More specifically: during both events magnified images of the source lie close to the Einstein ring of the lens, i.e. at $\theta \sim 1$ in each case; this corresponds to an optical depth of $40 \exp(-\kappa_0)$, which is $\simeq 4 \times 10^{-4}$ for the more distant lens, but $\simeq 4$ for the closer one, leading to substantial attenuation of the lensed images in the latter case. In other words, for sufficiently distant clouds the strongly magnified images are located at large physical separations from the cloud, and the lens can be regarded as effectively point-like.

5 DISCUSSION

The main barrier to the investigations we advocate is not so much the actual photometric monitoring, which is routine, but the identification of suitable targets. One approach which has previously been suggested (Walker & Ireland 1995; Tadros, Warren & Hewett 1998) is to monitor quasars lying behind rich clusters of galaxies at low redshift, but this approach is really only feasible for cameras which have exceptionally large fields of view. An alternative is to construct a very large sample of quasars, and then select out the small fraction which are viewed through halos of foreground galaxies, by cross-correlating with a galaxy catalogue.

We can estimate the microlensing optical depth which is contributed by galaxies within redshift z_d ($z_d < 1$) from $\tau(z_d) \sim \Omega_g z_d^2$ (c.f. Press & Gunn 1973), where Ω_g is the average mass per unit volume in galaxies, expressed in units of

the critical density, and we have assumed that galaxies are composed predominantly of microlenses. Taking $\Omega_g \sim 0.1$ it follows that we need a sample of $N_Q \sim 10^5$ quasars in order to amass a combined optical depth in excess of unity from galaxies within $z_d \simeq 10^{-2}$; no such sample exists. However, the dependence on redshift is quadratic, and within $z_d \simeq 0.02$ we need only $N_Q \sim 3 \times 10^4$ sources; so with the largest available quasar survey (Boyle et al. 1998) we expect a combined optical depth of $\tau(z_d = 0.02) \sim 1$. Of course the bulk of the quasars in any survey make a trivial contribution to this estimate, because they do not lie behind galaxy halos. If, for example, we suppose that each galaxy halo extends to a radius of 50 kpc, and we take the space density of galaxies to be $4 \times 10^{-3} \text{ Mpc}^{-3}$, then only 80 quasars contribute. Thus by selecting out the close angular coincidences between quasars and galaxies at low-redshift, it becomes feasible to monitor a sub-sample in which there is always a microlensing event in progress. At $z_d \lesssim 0.02$ the influence of the quasar dimensions on the observed light-curves should be small, provided the microlenses have masses $M \gtrsim 3 \times 10^{-5} M_\odot$ (see figure 1).

It is worth setting out the criteria by which microlensing can be distinguished from other causes of variability. Most importantly, for the proposed experimental conditions we expect only weakly chromatic light-curves for the optical continuum. If the lenses are sufficiently point-like then similar light curves are expected for the X-ray band, assuming that the X-ray source is comparable in size to the optical source. (But non point-like lenses introduce attenuation which may lead to X-ray extinction events — compare figs. 4 and 2.) However, one does not expect any associated changes in radio flux, because the emission region in this case is too large to be significantly affected. The same holds true for the optical emission lines, which are believed to arise from a region of much larger dimensions than the optical continuum. Note that for broad-band optical photometry this means there will always be a non-varying component required when fitting to theoretical light-curves. In this case one needs to subtract the steady, emission-line flux in each band prior to testing for achromaticity. For a single lens, and no strong external shear, one also expects the light-curves to be time-symmetric. These criteria can be employed for individual events. In addition, a strong test for microlensing becomes possible when a sample of candidate events is available: correlation of measured optical depth with the theoretical estimate. This correlation is expected to be good because the connection between theory (e.g. §2) and experiment is very close. This, coupled with the fact that intrinsic variations should have absolutely nothing to do with foreground objects — i.e. zero correlation predicted for intrinsic variations — makes for a very powerful test indeed.

6 CONCLUSIONS

It is desirable to initiate photometric monitoring of quasars seen through the outer halos of low-redshift galaxies. For this type of configuration, planetary-mass lumps of dark matter introduce discrete microlensing events which are unlikely to be confused with intrinsic outbursts. A strong test of any putative microlensing is available in the ensemble properties of the quasar sample: the measured optical depth should correlate well with the theoretical value. An observed correlation

of this type would eliminate the possibility of events being intrinsic to the sources, while non-detection could, for example, eliminate *all* Jovian-mass dark matter candidates — a conclusion which cannot be reached on the basis of LMC microlensing observations. If microlensing is indeed detected, the observed light-curves have the potential to differentiate between point-like lenses (black holes/planets) and gas clouds.

ACKNOWLEDGMENTS

Thanks to Mark Wardle, Brian Boyle and Ken Freeman for their thoughts on the various issues herein.

REFERENCES

- Alcock C. et al. 1997 ApJ 486, 697
 Alcock C. et al. 1998 ApJL 499, L9
 Baganoff F. K. & Malkan M. A. 1995 ApJL 444, L13
 Boyle B. J., Smith R. J., Shanks T., Croom S. M., Miller L. 1998 proc. IAU Symp. 183, Cosmological parameters and the evolution of the Universe
 Canizares C. R. 1982 ApJ 263, 508
 Carr B. 1994 ARAA 32, 531
 Dalcanton J. J., Canizares C. R., Granados A., Steidel C. C., Stocke J. T. 1994 ApJ 424, 550
 Draine B. T. 1998 ApJL 509, L41
 Fiedler R. L., Dennison B., Johnston K. J., Hewish A. 1987 Nat 326, 675
 Gerhard O. & Silk J. 1996 ApJ 472, 34
 Gott J. R. 1981 ApJ 243, 140
 Hawkins M. R. S. 1993 Nat 366, 242
 Hawkins M. R. S. 1996 MNRAS 278, 787
 Henriksen R. N. & Widrow L. M. 1995 ApJ 441, 70
 Irwin M. J., Webster R. L., Hewett P. C., Corrigan R. T., Jędrzejewski R. I. 1989 AJ 98, 1989
 Paczyński B. 1986 ApJ 304, 1
 Press W. H., Gunn J. E. 1973 ApJ 185, 397
 Refsdal S., Stabell P. 1993 A&A 278, L5
 Romani R., Blandford R. D. & Cordes J. M. 1987 Nat 328, 324
 Sahu K. 1994 Nat 370, 275
 Schild R. E. 1996 ApJ 464, 125
 Schmidt R. & Wambsganss J. 1998 A&A 335, 379
 Schneider P., Ehlers W., Falco E. E. 1992 Gravitational Lenses, Springer-Verlag, Berlin
 Tadros H., Warren S. & Hewett P. 1998 New Ast (astro-ph/9806176)
 Vietri M., Ostriker J. P. 1983 ApJ 267, 488
 Walker M. A., Ireland P. M. 1995 MNRAS 275, L41
 Walker M., Wardle M. 1998 ApJL 498, L125
 Wambsganss J., Paczyński B., Schneider P. 1990 ApJL 358, L33
 Zhao H. S. 1998 ApJL 500, L149

This paper has been produced using the Royal Astronomical Society/Blackwell Science \TeX macros.